Int J Adv Manuf Technol (2015) 80:1945–1955
DOI 10.1007/s00170-015-7144-9

ORIGINAL ARTICLE

Development and validation of a nonlinear dynamic impact model for a notch impact

Espen G. Lund[1] · Mladen Jecmenica[2] · Ole Melteig[2] · Kjell G. Robbersmyr[1] · Hamid Reza Karimi[1]

Received: 15 December 2014 / Accepted: 12 April 2015 / Published online: 1 May 2015

Abstract Finite element simulations are being more and more applied when studying the crash-worthiness of vehicles during impact. This paper deals with setting up such a simulation and discusses several ways to simplify and verify a simulated crash. For this purpose, a notch impact-testing machine will be released from a certain angle and crash into a model constructed with three different wall thicknesses. The plastic and elastic deformation is measured in the front of the model and is then used for validation of the simulation. In the end, the simulation was found to be in good agreement with the real crash data.

Keywords Dynamic impact · FEM simulation · Explicit simulation · Energy dissipation · Material damping

1 Introduction

Testing of an object's crashworthiness, for example, in the car industry, is usually executed by documenting and video-taping real crashes. However, testing in this manner can be very expensive, and it is usually a challenge to capture and observe how all components behave during crash. Being able to set-up a reliable simulation will have many advantages; the key ones being a much more detailed documentation of the crash and possible large savings on the expenses.

Dynamic impact simulations are most commonly either created by the finite element method (FEM) or by so-called lumped parameter models (LPM). A lumped parameter model is one or several masses in connection with springs and/or dampers. This will in turn generate a set of dynamic equations. The behaviour of the vehicle during impact can then be simulated by defining values for the spring- and damping coefficients. Although there are several mathematical models in the literature, Pawlus et al. [1] showed that the Maxwell model gives great results when compared with experimental crash data. Further, when dealing with LPMs, the spring- and damping coefficients almost certainly will need to be optimized to get satisfactory results. In Klausen et al. [2], they study the usefulness of the firefly optimization algorithm in a crash simulation based on a single mass. In Mitra et al. [3], the vehicle is modelled by a double spring-mass-damper system that represents the chassi of the vehicle and the passenger compartment. The model is validated by comparing the results from the model with the experimental results from real crash tests available.

LPMs are generally quite simplified and does not take into account any real properties, for example, geometry and material behaviour. Also, where LPMs can have as little as 1 degree of freedom, FEM models usually have several hundreds of thousands and contain much more detailed model properties. This means that acquiring a fully functional FEM simulation will generally be much more time consuming, of course depending on the complexity of the object. Previous work done on this subject can, amongst others, be found in Lund et al. [4] where the energy

This work was supported by the grant of the collaborative research project between the University of Agder and Telemark University College.

✉ Hamid Reza Karimi
hamid.r.karimi@uia.no

[1] Department of Engineering, Faculty of Technology and Science, University of Agder, 4879 Grimstad, Norway

[2] Institute for Process Technology, Department of Technology, Telemark University College, 3914 Porsgrunn, Norway

output of a dynamic impact is investigated. In Zaouk et al. [5], simulated crash results are compared with real crash footage and sensor data. In addition, the energy absorption by different components in a vehicle is discussed. Sun et al. [6] study the energy absorption of functionally graded structures with changing wall thickness. Fender et. al. [7] study substitute modelling where only the relevant mechanisms are simulated. Peng et al. [8] looked at the mechanical behaviour of windshield glass in the case of a pedestrian's head impact. Al-Thairy et al. [9] present the development of a simplified analytical method to predict the critical velocity of transverse impact by rigid body on steel column under axial load. Liao et al. [10] optimized a vehicle design to increase the energy absorption during frontal and oblique crash. Kim et al. [11] optimize the energy absorption with respect to the size of the motor room. In Kirkpatrick et al. [12], a Ford Crown Victoria is subject to a tear-down, and all the important structural components are digitalized. To validate the model, component crash tests were performed which allowed validation of different vehicle components prior to the full vehicle crash. In Zaouk et al. [13], they demonstrate an initial step at learning how to develop smaller vehicle models for simulation purposes. Yehia et al. [14] study vehicle-to-light-post impact situations with different light post materials. In Dasgupta et al. [15], they propose a method of finding meaningful damping values for multi-degree of freedom systems. Borovinvsek et al. [16] present full-scale crash tests were the results are compared with real crash data. In Ramon et al. [17], advanced techniques are presented from the importance of the mesh quality. In Marzougui et al. [18], model validation focuses on the comparison of the test and simulations in terms of crush depth in the front of the vehicle. Lastly, Simulia Abaqus [19] has been a very helpful literature with their extensive user guide giving theoretical information regarding the theory of the finite elementbreak method.

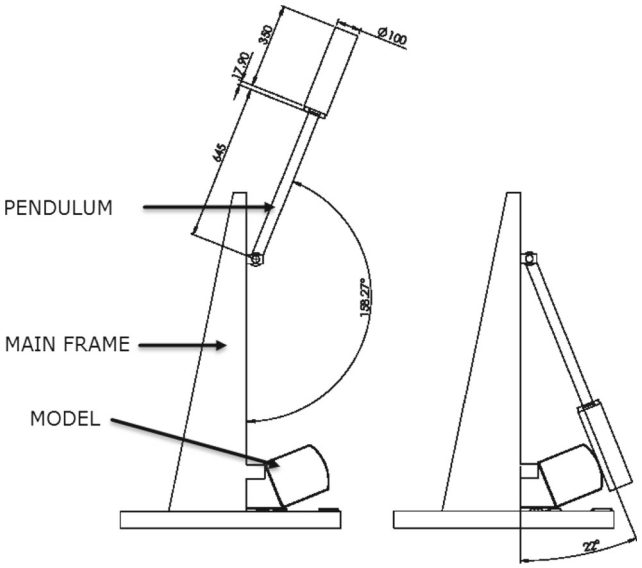

Fig. 2 The notch impact set-up. Starting position before the pendulum is released is seen to the left and impact position is seen to the *right*

In this paper, a finite element simulation of a notch impact machine is described in detail. The model subject to the impact is constructed with three different wall thicknesses. The depth of the deformation in the front of each model is then compared with real crash data. In addition, the paper investigates the usefulness of the Rayleigh Damping as a damping model in nonlinear impacts. It also suggests several ways to simplify a simulation, for example, ways to reduce the number of degrees of freedom, thus saving computational time, as well as methods of shortening the simulation time. Furthermore, the paper gives different ways to verify a simulation. This involves investigating the energy output of the crash and the effect of the mesh size on the deformation. Lastly, the simulation results are found to be in good agreement with the crash test data.

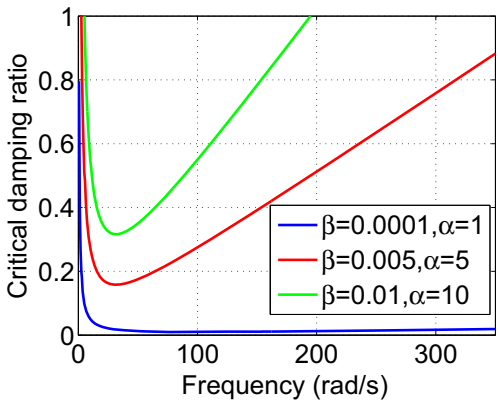

Fig. 1 The Rayleigh damping curve for different values of α and β

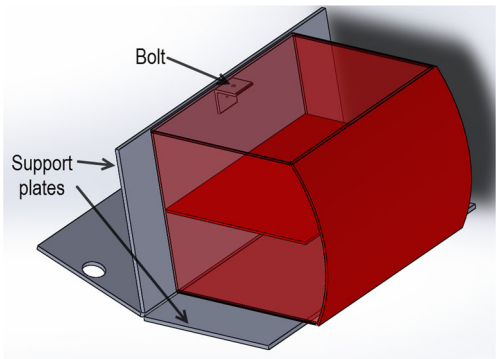

Fig. 3 The model resting on the support plates. The model is made transparent for clarity

Table 1 Deformation of the three models

Thickness [mm]		Plastic + elastic [mm]	Plastic [mm]	Elastic [mm]
t1:	3	16.57	11.20	5.47
t2:	2	28.80	24.50	4.30
t3:	1.5	34.33	31.5	2.83

2 Theoretical background

2.1 The finite element method

In the finite element method , the equation of motion of a discretized structure is presented as follows

$$M \cdot \ddot{u} - P + I = 0 \tag{1}$$

where M is the mass matrix of the structure, $\ddot{u}$ is the node acceleration matrix, and P and I are the applied and internal forces, respectively. If there is damping in the model, the internal force becomes

$$I = K \cdot u + C \cdot \dot{u} \tag{2}$$

where K is the structure stiffness matrix and C is the structure damping matrix. In this case, the equation is solved explicitly due to large nonlinearities caused by rapid changes in contact, large deformations and material non-linearities. The stability limit, that is the largest possible time step the solution can have and still remains stable, is chosen automatically by the simulation software.

where the parameters α and β are known as the mass proportional and stiffness proportional damping constants, respectively. For any given mode, i, the damping ratio—meaning the ratio between a harmonic oscillating and critical damped system—is defined as in Eq. 3:

$$\zeta_i = \frac{\alpha}{2 \cdot \omega_i} + \frac{\beta \cdot \omega_i}{2} \tag{3}$$

where ζ_i is the damping ratio and ω_i is the frequency for any given mode shape.

As can be seen directly from the equation, α is dominant at low frequencies while β is dominant at high frequencies. This is further emphasized in Fig. 1 where the Rayleigh damping model is plotted three times. Each plot has different parameter values for α and β to illustrate the effect of each parameter.

When solving explicitly, it is not possible to define a damping ratio for each mode frequency, which, on the contrary, is possible for implicit solvers. Therefore, some modes will be damped more and some less. Consequently, it is important to be aware of which mode shapes that are the most influential to the response of the structure and that the damping ratio is closest to the desired damping at these frequencies. If the first three mode shapes are of little influence, then, it really does not matter if these modes are not reasonably damped because it will not greatly affect the response of the structure [19].

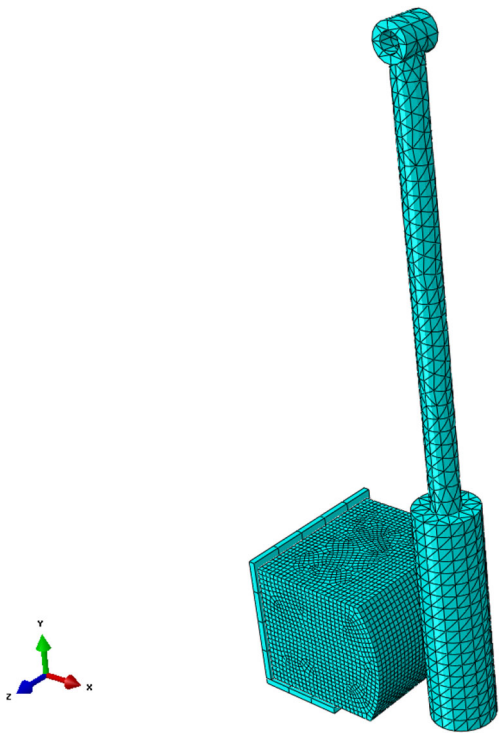

Fig. 4 The finite element model

2.2 Energy balance

The total energy balance of a system, TE, can be written as Eq. 4

$$TE = IE + VDE + FDE + KE \tag{4}$$

where IE is the internal energy (defined in Eq. 5) and VDE is the viscous dissipated energy. Viscous dissipated energy is energy dissipated through damping mechanisms,

Table 2 Comparison of velocity at moment of impact between video of real crash and the simulation

From video [rad/s]	From simulation [rad/s]
6.7766	6.7275

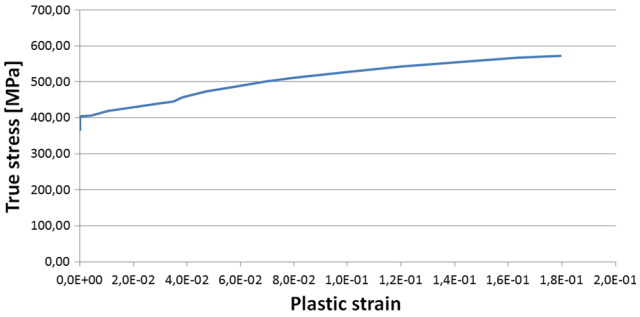

Fig. 5 True stress vs. plastic strain

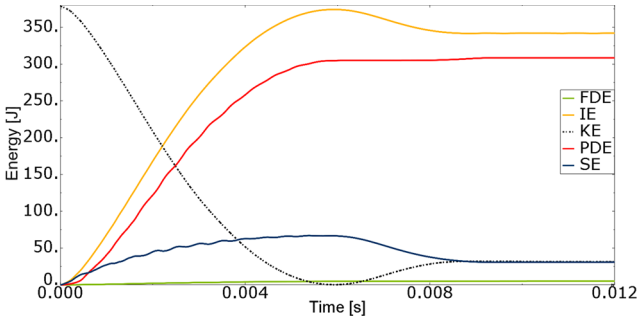

Fig. 6 Energy output of the model with a thickness of 3 mm

e.g. material damping and bulk viscosity. Further, FDE is the energy from friction between surfaces and KE is the total kinetic energy of the structure.

The internal energy can be given as follows

$$IE = SE + PDE + AE \tag{5}$$

where SE is elastic strain energy, PDE is energy dissipated through inelastic processes (after material yielding) and AE is artificial strain energy. Artificial strain energy is energy used by the computer software to control hourglass deformation in the elements [19]. In other words, high levels of artificial strain energy will result in possible large errors and should therefore be as low as possible. This energy can easily be reduced by refining the structure's mesh at critical areas. This will, however, further increase the simulation time because in explicit simulations, the simulation time is mainly dependent on the size of the element mesh.

3 The notch impact set-up

In order to have real crash data for comparison with the FEM simulation, a notch impact machine was assembled (Fig. 2). The whole set-up consists of the main frame, a pendulum and a crash test model. The crash test is initiated by releasing the pendulum from a certain angle (left position) and letting it crash into the model (right position).

The crash test model was constructed with 3-, 2- and 1.5-mm wall thicknesses. These three models were all subjected to the same impact scenario, as presented in the figure above. Each crash was then video-taped by a high-frame video camera. Then, after each crash, the depth of the plastic deformation was measured from the curved front plate.

In the set-up, the model is resting on two support plates with a bolted connection to the rear support plate (Fig. 3). The model also has a center plate welded to its side plates.

The plastic deformation in front of the model was measured using a calliper. To measure the elastic deformation, three markers were placed on the pendulum with a defined distance between them. The middle marker was placed exactly where the pendulum would hit the model. A tracking function was then used to draw a red line from the middle marker right at the moment of impact to the moment of maximum deformation. This red line could then be scaled and used for measuring the deformation, using the known distance between the markers as a reference. When solving the simulation explicitly, material damping can be introduced by Rayleigh damping which is defined in Eq. 6

$$C = \alpha \cdot M + \beta \cdot K \tag{6}$$

The measured results from all three crashes are summarized in Table 1. The three models are hereby denoted t1, t2 and t3.

4 Modelling and analysis

The finite element representation of this set-up is simplified to containing the pendulum, the support plates and model (Fig. 4). The model is created using shell elements. This

Table 3 The effect of artificial energy on the maximum displacement

Mesh [mm]	E_I [J]	E_A [J]	$\frac{E_A}{E_I} \cdot 100$ [%]	$D_{\max}$ [mm]
20	337.5	11.8	3.5	18.7
15	341.1	8	2.3	19.1
10	341.7	4.2	1.2	19.5
9	341.6	3.2	0.9	19.6
8	341.8	2.83	0.8	19.6

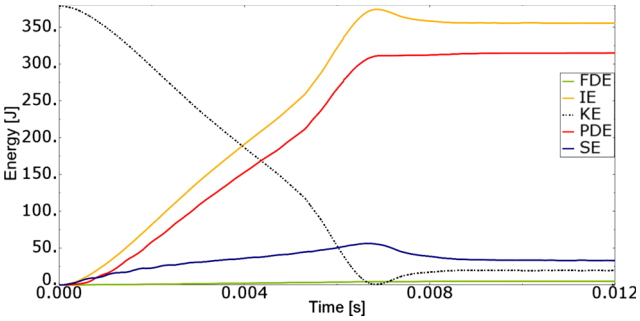

Fig. 7 The energy output of the model with a thickness of 2 mm

reduces the number of nodes and consequently shortens the computational time. It is also an efficient way to change the wall thickness without having to re-create the entire finite element model for each thickness. However, shell elements should only be used if the ratio of the thickness, t, divided by the plate length, L, is lower than 0.1.

$$\frac{t}{L} < 0.1 \tag{7}$$

The pendulum and the support plates are regarded as so-called rigid elements. In doing so, motion of all nodes are governed by a single reference point. For the pendulum, this reference point is placed in the rotation center. This point has all its degrees of freedom locked except for rotation around the z-axis. The reference point for the support plates has all its degrees if freedom locked. This greatly decreases computational time as all the nodes' DOFs in the rigid components are now reduced to two reference points. This modelling method is only valid if the rigid components are much stiffer than the other components and that they consequently will have no deformation during the impact.

Furthermore, the simulation is simplified to be initiated right at the moment of impact. This is done because it is only the impact itself that is of interest. The time period the pendulum uses to reach the model is therefore not part of the simulation. Such simplifications can greatly reduce the simulation time. However, it should only be done if there are ways to validate the initial velocity used in the simulation. In this paper, this is achieved

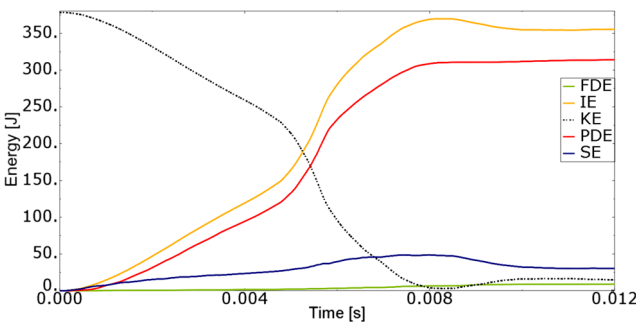

Fig. 8 The energy output of the model with a thickness of 1.5 mm

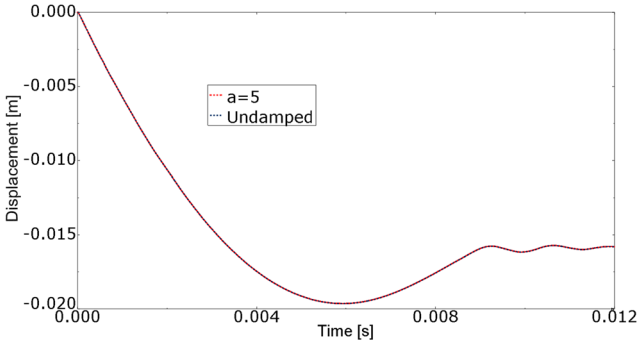

Fig. 9 Damped (α) vs. undamped displacement of the 3 mm model

by reading the rotation velocity of the pendulum, ω, from a high-frame video of the impact. In order to verify the simulation set-up, a single simulation was run with the pendulum being released from its initial position (recall Fig. 2). The velocity from the simulation was then compared with the video. Evidently, the simulated velocity fits very well with the velocity obtained from the video (Table 2).

Regarding material properties, the model is meeting requirements of EN10149-2 S355MC. For impact simulations, an accurate material model is essential. Therefore, a tensile test of the material was conducted. The results from the test give the elongation of the test specimen and the corresponding tensile load. These results can, in turn, be calculated into nominal strain and nominal stress. These values are, however, based on the test specimen's original cross sectional surface area but can be calculated to true stress and true strain by the following set of equations:

$$\epsilon = ln(1 + e) \tag{8}$$

$$\sigma = R \cdot (1 + e) \tag{9}$$

where ϵ is the true strain, e is the nominal strain, σ is the true stress and R is the nominal stress. It varies, depending on the type of computer software, what type of strain and stress it takes as input for the material model. Abaqus, which is used

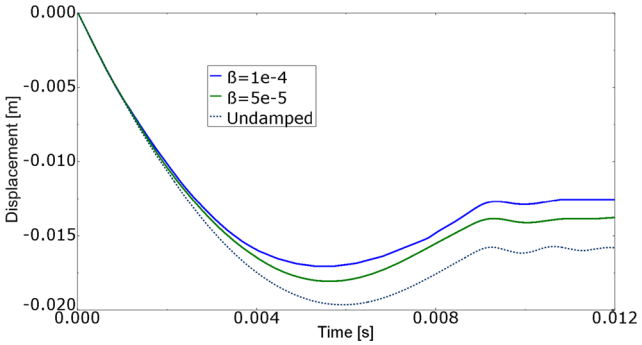

Fig. 10 Damped (β) and undamped displacement of the 3-mm model

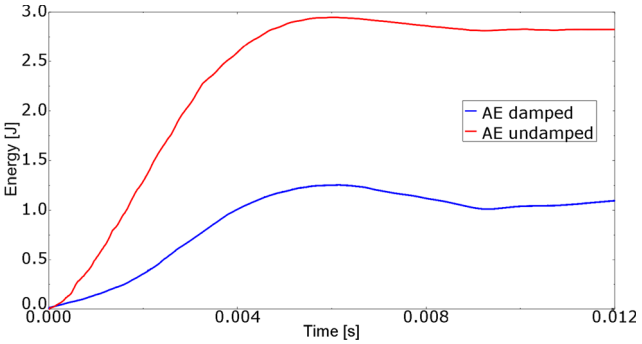

Fig. 11 Hourglass energy is reduced by introducing material damping

in this paper, uses true stress and plastic strain as inputs. The plastic strain can be calculated as follows:

$$\epsilon_p = ln(1+e) - \frac{\sigma}{E} \tag{10}$$

where E is the material's elastic modulus. Finally, the true stress vs. plastic strain can be plotted (Fig. 5).

In addition, general material parameters for the model are the following:

- ρ=7800 $\frac{kg}{m^3}$
- σ_{ys} = 355 MPa
- E = 210 GPa
- ν = 0.3

where ρ is the mass density of the material, σ_{ys} is the yield stress and ν is Poisson's ratio.

The contact formulation used in the simulation is Abaqus' *general contact* for all components. It is known to be a robust formulation and as accurate, or even better, than normal contact pair definitions [20]. For normal contact, the formulation applies a penalty-based formulation where the resulting friction force, F_{fr}, is the friction coefficient, μ, times the normal force, N (11). For steel against steel, the friction coefficient is 0.3. The tangential behaviour is defined as *hard contact*.

$$F_{\text{fr}} = \mu \cdot N \tag{11}$$

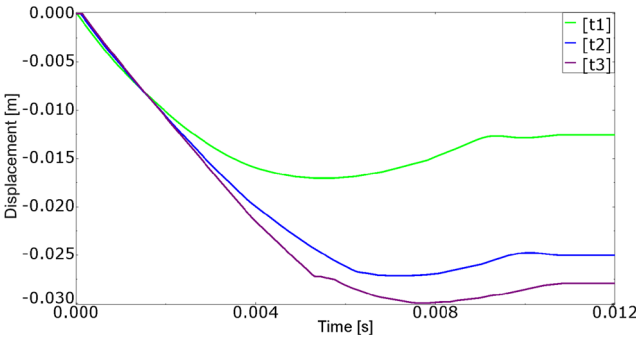

Fig. 12 Damped displacement plots

Table 4 Simulated deformations in front of the model

Model	Plastic + elastic [mm]	Plastic	Elastic
t1	17.04	12.50	4.54
t2	27.13	25.00	2.13
t3	30.00	28.00	2.00

5 Results

As mentioned, in order to control hourglass deformation in first-order reduced integration elements, a portion of the internal energy of the system goes to hourglass resistance. There are several ways of reducing this energy, mainly by adding a damping viscosity to the elements or simply refining the mesh. In the case of dynamic impacts, where the displacement is of interest, it is interesting to see how low this energy must be in order for the solution to converge. Therefore, a mesh convergence test on the model with 3-mm wall thickness was executed. The mesh density was increased to see the change in artificial energy and maximum displacement D_{max} (Table 3). Observably, the maximum displacement converges to 19.6 mm when the artificial energy becomes below 1 % of the internal energy. Therefore, an average mesh size of 8 mm is used on all three models.

Figure 6 plots the rest of the energy output for the same simulation. In addition to the artificial energy, the viscous dissipated energy is excluded from the plot because the magnitude is negligible compared to the others. The viscous dissipated energy exist because Abaqus, by default, introduces material damping in the form of bulk viscosity in order to damp very high frequency responses.

The kinetic energy at the moment of impact is 378.4 J. To further validate the model, the kinetic energy is also calculated by hand. Evidently, the two values correspond very well (12):

$$\text{KE} = \frac{1}{2} \cdot J \cdot \omega^2 = \frac{1}{2} \cdot 16.6\, kgm^2 \cdot 6.7722 \frac{rad}{s} = 380.7\ \text{J} \tag{12}$$

where J is the pendulum's moment of inertia around its rotary axis.

As the pendulum crashes into the model, the pendulum's kinetic energy is transformed to mainly deformation energy. The largest portion of this deformation energy stems from the plastic dissipated energy (90.2 %), while a smaller portion comes from the elastic strain energy (8.9 %). The rest of the energy is the artificial energy. The strain energy has a small peak at the moment of maximum crush. This peak, however, falls afterwards as the elastic deformation recovers.

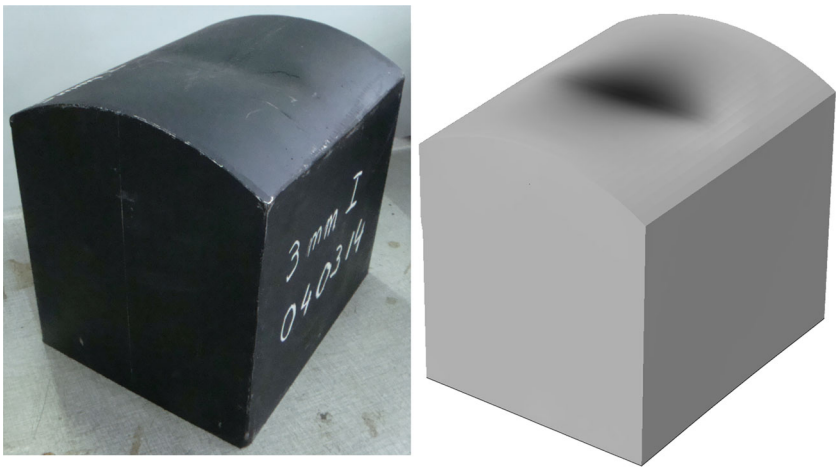

Fig. 13 Real vs. simulated deformation of the 3-mm model (iso view)

Fig. 14 Real vs. simulated deformation of the 3-mm model (front view)

Fig. 15 Real vs. simulated deformation of the 3-mm model (top view)

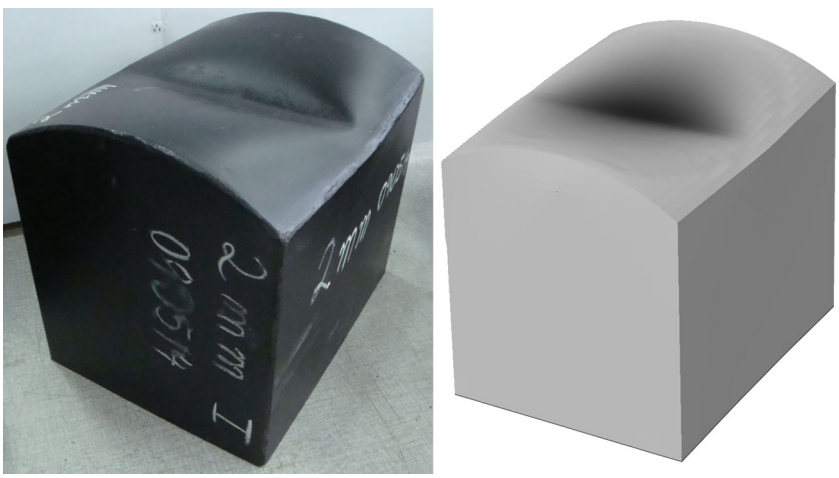

Fig. 16 Real vs. simulated deformation of the 2-mm model (iso view)

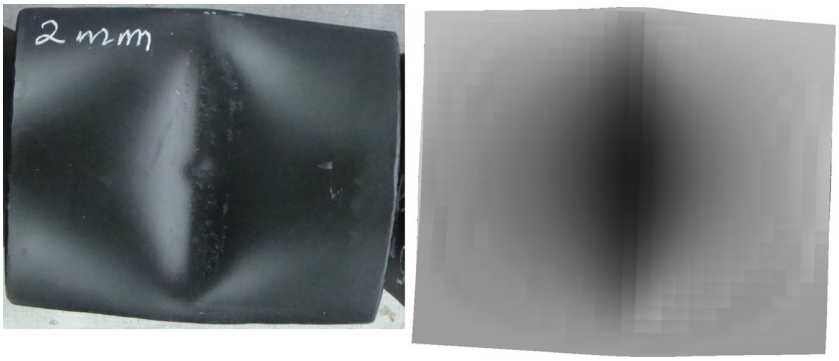

Fig. 17 Real vs. simulated deformation of the 2-mm model (front view)

Fig. 18 Real vs. simulated deformation of the 2-mm model (top view)

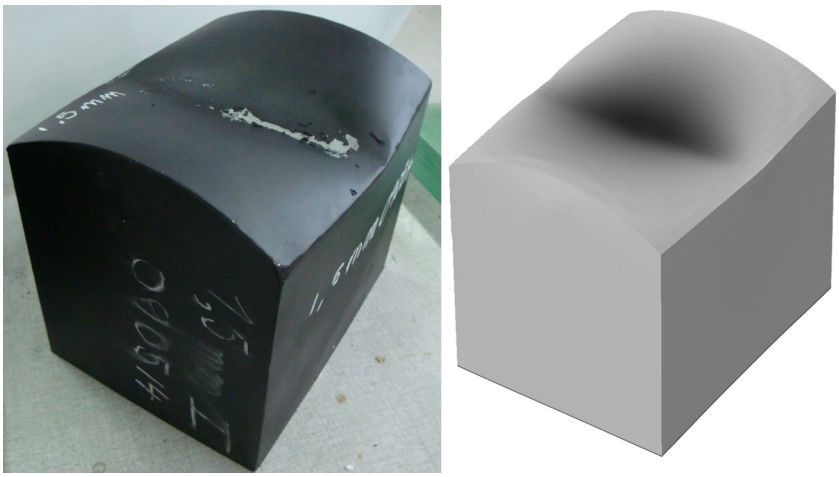

Fig. 19 Real vs. simulated deformation of the 1.5-mm model (iso view)

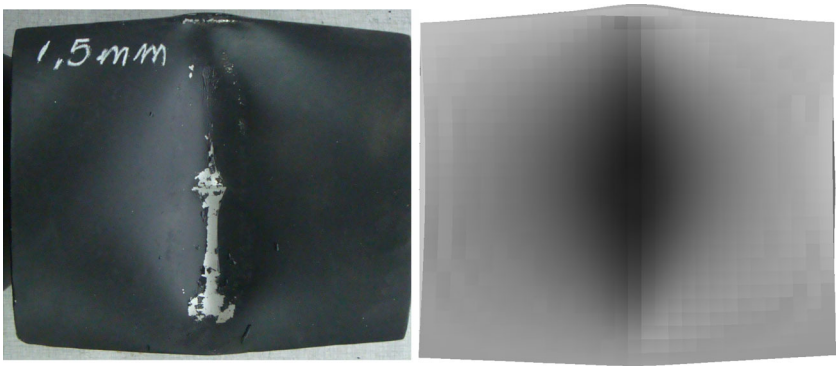

Fig. 20 Real vs. simulated deformation of the 1.5-mm model (front view)

Fig. 21 Real vs. simulated deformation of the 1.5-mm model (top view)

Observably, the energy plot of the 2-mm model (Fig. 7) shows that the ratio of plastic dissipated energy (88.6 %) and elastic strain energy (9.2 %) stays approximately the same. Again, the rest of the energy is artificial energy.

Also for the 1.5 mm model, the ratio of kinetic energy dissipated by inelastic (88.4 %) or elastic energy (8.5 %) is almost identical to the two previous impact simulations (Fig. 8).

Furthermore, some energy should be dissipated through material damping. As mentioned, material damping is introduced in explicit simulations by Rayleigh damping, which is defined by the parameters α and β. These values can be difficult to define, especially for finite element systems with several hundreds of thousands of degrees of freedom. In order to observe the influence of each parameter, a parameter study on the 3-mm model was conducted. As can be seen, a damping parameter of $\alpha = 5$ barely affects the plot at all (Fig. 9), even though that a damping value of $\alpha = 5$ is regarded as a pretty high value. On the other hand, β greatly affects the displacement plot (Fig. 10). This could indicate that β is a dominant Rayleigh damping parameter for impact simulations and that the mode shapes with the highest frequencies are the most influential. Also, contrary to intuition, introducing material damping greatly increases the simulation time as it reduces the stable time increment of the simulation. It is therefore probably wise to include it first after initial testing of the model.

What can also be seen from the displacement plots above is that without material damping in the model (Fig. 11), the nodal displacement will oscillate, even after all the elastic deformation has recovered. This is, intuitively, cancelled out by a higher damping factor. A damping coefficient of $\beta = 10^{-4}$ removes the oscillations.

The introduction of material damping interestingly enough also decreases the artificial energy quite significantly, as can be seen from Fig. 12. This is probably caused by that the damping parameter β is multiplied by the element stiffness matrix and thus help to reduce the hourglass phenomenon.

In the end, as mentioned, a damping coefficient of $\beta = 10^{-4}$ gave good results (Table 4). Recalling the measured deformations of the real crash models (Table 1), the results match very well.

Finally, pictures comparing the real- and simulated deformations are presented. The real- and simulated plastic deformation of the 3-mm model match very well (Figs. 13, 14 and 15). The same goes for the 2 mm where the deformation is nearly spot on (Figs. 16, 17 and 18). Regarding the 1.5-mm model, the deformation is just under 4 mm larger in the real model than the simulation results. However, the deformation shape is very similar. Especially encouraging is the visible curving of the top plate (Figs. s19, 20 and 21).

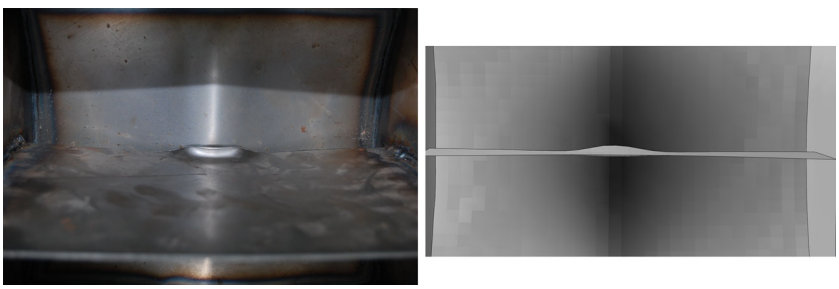

Fig. 22 Real vs. simulated deformation in the center plate of the 1.5-mm model

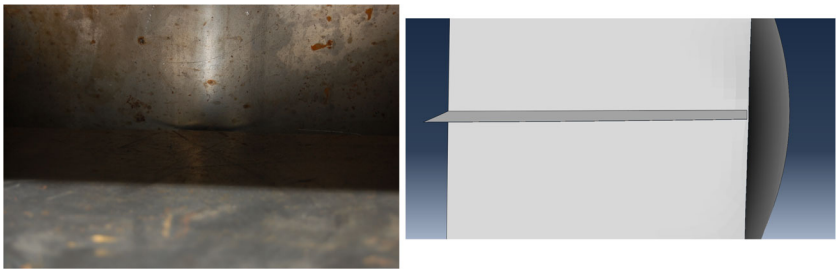

Fig. 23 Real vs. simulated deformation in the center plate of the 2-mm model

In the real crash, the center plate made contact with the curved front plate at both the 2- and 1.5-mm models (Figs. 22 and 23, respectively). The deformation of the 1.5-mm model's center plate is, of course, a bit lower in the simulation compared to the real model because of lower deformation in the curved front plate. However, the simulation has captured a very similar shape. Regarding the 2-mm model, it is clear that there has been contact because of the visible mark on the curved front plate. However, this has only resulted in elastic deformation in the center plate, as there is no visible deformation after the crash. From the simulation, because there is 1 mm less plastic and elastic deformation in the curved front plate, the center plate barely misses contact.

6 Conclusions

In this paper, it was concluded that, for impact simulations, the lion's share of the internal energy should stem from plastic dissipated energy. From the results, the plastic dissipated energy should be, of course depending on material properties, etc, in the area of 90 % of the internal energy. Also, a sufficiently fine mesh is critical for high velocity impact simulations. A coarse mesh will lead to energy being dissipated by hourglass control and lead to possible large errors. Hence, the artificial energy should only be a very low amount of the internal energy, preferably below 1 %. While it can be reduced by refining the element mesh at critical areas, this will also significantly increase the computational time of the simulation. In addition to refining the mesh, it was found that introducing material damping in the form of Rayleigh damping further decreases the artificial energy.

Rayleigh damping is an efficient material damping model with, for impact simulations, only one parameter to tune. For impact simulations with a high frequency response, the Rayleigh damping parameter β is dominant and α has little to none effect on the displacement plot. It has also been seen that the same parameter value gives good results on different models. Material damping reduces the total deformation and eliminates oscillations after the elastic deformation is fully recovered. Contrary to intuition, material damping greatly increases the simulation time.

The simulation results are found to be in good agreement with the crash test data.

References

1. Pawlus W, Karimi HR, Robbersmyr KG (2014) Investigation of vehicle crash modeling techniques: theory and application. Int J Adv Manuf Technol 70(5-8):965–993
2. Klausen A, Tørdal SS, Karimi HR, Robbersmyr KG, Jecmenica M, Melteig O (2014) Firefly optimization and mathematical modeling of a vehicle crash test based on single-mass. J Appl Math 2014:10. Article ID 150319
3. Mitra AC, Benerjee N (2014) Vehicle dynamics for improvement of ride comfort using a half car bondgraph model. Int J Res, Sci Developers 2:1–5
4. Lund EG, Jecmenica M, Karimi HR, Robbersmyr KG, Melteig Ole (2014) Energy analysis of a non-linear dynamic impact using FEM. Proceeding of the 11th World Congress on Intelligent Control and Automation, Shenyang, China, pp. 6075–6080.
5. Zaouk AK, Bedewi NE, Kan C-D, Marzougui D (1996) Validation of a non-linear finite element vehicle model using multiple impact data. ASME Appl Mech Div-Publ-Amd 218:91–106
6. Sun G, Fengxiang X, Li G, Li Q (2014) Crashing analysis and multiobjective optimization for thin-walled structures with functionally graded thickness. Int J Impact Eng 64:62–74
7. Fender J, Duddeck F, Zimmermann M (2014) On the calibration of simplified vehicle crash models. Struct Multidiscip Optim 49(3):455–469
8. Peng Y, Yang J, Deck C, Willinger R (2013) Finite element modeling of crash test behavior for windshield laminated glass. Int J Impact Eng 57:27–35
9. Al-Thairy H, Wang YC (2013) A simplified analytical method for predicting the critical velocity of transverse rigid body impact on steel columns. Int J Impact Eng 58:39–54
10. Liao X, Li Q, Yang X, Zhang W, Li W (2008) Multiobjective optimization for crash safety design of vehicles using stepwise regression model. Struct Multidiscip Optim 35(6):561–569
11. Kim B-Y, Jeong C-M, Kim S-W, Suh M-W (2012) A study to maximize the crash energy absorption efficiency within the limits of crash space. J Mech Sci Technol 26(4):1073–1078
12. Kirkpatrick SW, Simons JW, Antoun TH (2000) Development and validation of high fidelity vehicle crash simulation models. SAE Trans 109(6):872–881
13. Zaouk AK, Bedewi NE, Kan C-D, Marzougui D (1996) Development and evaluation of a c-1500 pickup truck model for roadside

hardware impact simulation. In: Proceedings of the FHWA vehicle crash analysis crash conference. Citeseer, Mclean, VA, pp 1–31
14. Abdel-Nasser MAKAY, Alrajhi J (2013) Frontal crash simulation of vehicles against lighting columns in Kuwait using FEM. Int J Traffic Trans Eng 2:101–105
15. Chowdhury I, Dasgupta SP (2003) Computation of Rayleigh damping coefficients for large systems. Electron J Geotech Eng 8(0)
16. Borovinšek M, Vesenjak M, Ulbin M, Ren Z (2007) Simulation of crash tests for high containment levels of road safety barriers. Eng Fail Anal 14(8):1711–1718
17. Ramon-Villalonga L, Enderich Th (2007) Advanced simulation techniques for low speed vehicle impacts. Proceedings of 6th LS-DYNA
18. Marzougui D, Kan C-D, Bedewi NE (1996) Development and validation of an NCAP simulation using LS-DYNA3D. FHWA/NHTSA National Crash Analysis Center, The George Washington University, Virginia Camnpus, Virginia, USA
19. Simulia. Getting started with Abaqus: interactive edition
20. Tony Richards Stephen King. Solving contact problems with abaqus. Simulia